Controlled Deposition of Polymer Coatings on Cylindrical Photonic Devices

Amado M. Velázquez-Benítez, Moisés Reyes-Medrano, J. Rodrigo Vélez-Cordero, and Juan Hernández-Cordero, *Member, IEEE*

***Abstract*—We present a simple system for coating cylindrical devices for photonic related applications based on a wire coating method. Characterization of the system was done using two different polymeric materials, silicon-based PDMS and an acrylate-based polymer, obtaining different coating thicknesses upon varying the parameters of the process. Layers with controlled thickness ranging from hundreds of nanometers to 1 mm can be readily applied over devices with different diameters. We demonstrate the system capabilities for coating tapered optical fibers and glass capillaries. The fabrication of a tunable fused fiber coupler with a photoresponsive polymer layer is also demonstrated.**

***Index Terms*—Optical devices, optical fibers, optical fiber sensors, photothermal effects, polymers, thermooptic effects, thin films.**

I. Introduction

FUNCTIONAL coatings have been a major subject in optics and a key factor for the fabrication of optical devices. In general, coating films in optics are required to be smooth and uniform, features that are typically achieved with a highly controllable deposition process. Thin layers of solid materials represent the preferred choice for coatings and these are typically deposited over substrates by means of plasma-assisted or chemical methods (e.g., PVD, CVD, sputtering, etc.) [1]–[3]. Different surfaces and geometries can be uniformly coated with these methods relying on highly specialized equipment for achieving the desired optical features.

The use of polymers for coatings provides major advantages over other materials because of their lower fabrication costs and ease of processing. Simpler methods to create coating layers are also available when employing fluidic materials. The most common methods for applying liquid coatings include spin coating, dip coating, and roll coating, and the features of the resulting layers rely on the physical properties of the coating material. These methods are limited to planar surfaces, making them hard to apply on other geometries [4]–[6]. Spray coating has been used over small sections of wires of different materials (e.g., optical fibers [7]) but the resulting layers are neither sufficiently smooth nor uniform, thereby yielding optical losses.

Manuscript received September 15, 2014; revised November 7, 2014; accepted November 23, 2014. Date of publication December 3, 2014; date of current version January 23, 2015. This work was supported in part by DGAPA-UNAM under Grant PAPIIT-IN102112.

The authors are with the Instituto de Investigaciones en Materiales, Universidad Nacional Autónoma de México, Copilco, Ciudad de México 04510, DF, México (e-mail: amadovelb@gmail.com; e.moisesrm@gmail.com; jvelez@iim.unam.mx; jhcordero@iim.unam.mx).

Color versions of one or more of the figures in this papers are available online at http://ieeexplore.ieee.org.

Digital Object Identifier 10.1109/JLT.2014.2377173

In general, uniform coatings on cylindrical surfaces are challenging due to the geometry and the processes currently available are aimed at coating large lengths of material [8], [9]. However, coating cylindrical elements of reduced diameter with thin and uniform layers of polymeric materials is required in waveguide-based photonic devices. As an example, evanescent wave fiber optic sensors usually require thin layers of the sensitive material to provide adequate interaction of the evanescent field [10]. Molding techniques for coating are the most popular for these applications, but mold fabrication can be a challenging task [11], [12]. More versatile techniques are based on variations of the dip coating process, using a drop of the coating fluid that moves along a tapered fiber leaving a layer of the material on the waveguide surface [13], [14]. Polymeric materials commonly employed in the fields of optics and photonics are based on acrylate, styrene, carbonate, and silicone compounds [15]. Applications for these materials are defined according to their characteristics and properties such as refractive index, hardness, and thermal effects, just to name a few.

In this paper we present a system for applying polymer coatings on small cylindrical devices intended for photonic applications. The system versatility allows for single layer coatings with thicknesses ranging from 500 nm and up to 50 microns upon controlling the velocity of the coating process (0.375 to 5.71 mm/min). Furthermore, the proposed system is also capable of coating devices with diameters as small as 1 micrometer and up to 1 millimeter. Two coating materials are evaluated: one based on silicone oil and one based on acrylate; thus, we assess the performance of the coating system using materials with different properties like viscosity (0.5 to 6.45 Pa/s) and surface tension (19.8 to 36.09 mN/m). Polymer coatings of controlled thicknesses are applied on single-mode tapered optical fibers and we further demonstrate coating of cylindrical channels intended for microfluidic applications such as flow control in capillary glass tubes. As a practical example, we demonstrate that a photo-responsive polymer can be readily applied on a fused fiber optic coupler thereby yielding an optically tunable device.

II. Theoretical Background

Our approach for coating cylindrical optical devices is based on the principles of wire coating. When pulling a wire of constant diameter and smooth-uniform surface through a liquid solution, a small amount of the liquid coats the wire; the thickness of the coating layer depends on the intrinsic properties of the liquid. Features of the liquid such as viscosity (η) and surface tension (γ) play a very important role defining the resulting

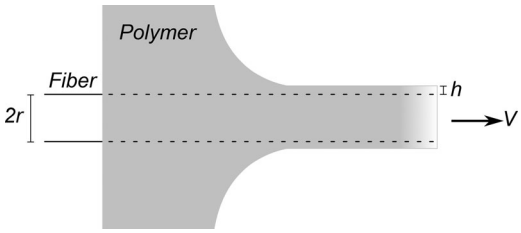

Fig. 1. Wire coating principles: the wire (radius r) is pulled at a constant velocity (V) through a liquid container and a layer of liquid material (thickness h) is left on the surface of the wire.

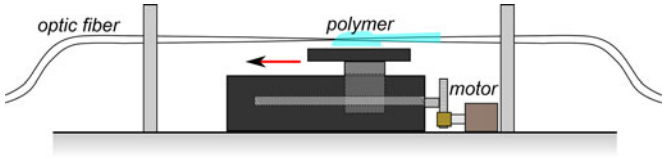

Fig. 2. Schematic representation of the system for coating cylindrical optical devices.

coating layer. Landau, Levich, and Derjaguin (LLD) first described this process for wire coating [16], and Ryck and Quéré described the dynamics of the process [17], [18]. The resulting layer thickness (h) on a wire of radius r (see Fig. 1) can be estimated as:

$$h = 1.34 r Ca^{2/3} \tag{1}$$

$$Ca = \eta V/\gamma \tag{2}$$

where Ca is the capillary number and V is the velocity at which the process takes place. This expression is only valid for $Ca << 1$, which implies that $h < r$. For values of Ca close to 1, adjustments on (1) are made considering an equivalent radius $r + h$ instead of only r, as proposed by White and Tallmadge [19].

When a wire is coated with a liquid, the resulting layer tends to be unstable and undulates, an effect described by the Plateau-Rayleigh instability [20]. Such effect generates a series of periodic droplets growing with a characteristic time (t_0) given by:

$$t_0 = 12 \frac{\eta (r+h)^4}{\gamma h^3}. \tag{3}$$

From Eq. (3), it can be seen that the growth of this instability depends on the wire and the coating thicknesses. For the case when h is small compared to r, the required time for instability formation will be large. On the other hand, for large h, the instability will appear a few seconds after the coating layer has been deployed, thus producing a non-uniform coating. Instability formation is therefore a very important factor in wire coating since its characteristic growth time will limit the size of the uniform layer that can be formed with this approach. If polymers are sought as coating materials, the instability growth time must be larger than the time required for the curing process of the polymer in order to obtain a uniform coating layer. Gravity effects could be a cause of radial variations, and these can be gauged upon comparing capillary and gravity forces using the Bond number, given by:

$$Bo = \frac{\rho g r^2}{\gamma} \tag{4}$$

were ρ is the density of the liquid polymer and g is the gravity acceleration. For $Bo \ll 1$, gravity effects can be neglected and thus radial uniformity on the coating layer can be assumed; otherwise the deposited layer thickness will depend on the capillary and Bond numbers [18]. As described in the following section, coating of cylindrical optical devices can be readily achieved with a variation of the wire coating technique.

III. System Design and Construction

The coating system was designed to provide the flexibility to accommodate devices ranging from one micron in diameter (e.g., single-mode tapered optical fibers) up to a millimeter (e.g., glass capillary tubes). In general, wire or fiber coating is performed upon pulling them through a container where the liquid solution is allocated, and the output diameter of the container determines the thickness of the coating. However, this technique requires large lengths of fiber and induces some strain, thus representing a problem when fragile optical devices are used. In order to avoid rupture or deformation of tapered fibers, our coating system relies on maintaining the fiber fixed and moving the coating fluid along the section to be coated. Once the fiber is fixed, a small section is immersed in the coating solution, which is contained inside a small fluid reservoir. This is finally displaced along the fiber at a controlled velocity in order to obtain a uniform coating thickness. The basic structure of the system is formed by two supports for holding the fiber, one motorized translation stage and a reservoir for the liquid coating material. A schematic representation of the coating system is shown in Fig. 2.

A stepper motor mechanically coupled through gears provides the displacement of the translation stage for depositing the liquid coating. Upon adjusting the step sequencing, the displacements that can be achieved by two different sets of gears comprise 125 or 250 nm per step and 2 or 4 μm per step, where both displacements for every gear are achieved using the half and full step sequencing, respectively. For the two sets of gears used in our experiment, the maximum velocity was 2 and 24 mm/min. The displacement and velocity of the stage is controlled through a microprocessor used for adjusting the time delay between the steps of the motor.

The reservoir for the coating material is a PTFE bar with U-shaped grooves serving as the liquid container and as the mobile section of the system. Full immersion of the devices in the liquid coating is achieved upon placing them at the center of the U-grooves, which have a length of 6.5 mm and a cross sectional area of 1.5 $\times$ 2 mm^2 (width and depth, respectively). The position of the PTFE bar can be adjusted manually at any section along the device prior to the coating process. As illustrated in Fig. 3, optical fibers are held in place horizontally and aligned by means of two identical metallic bars with parallel grooves and magnetic holders. Positioning of the fibers/capillaries is done manually upon applying the appropriate tension to avoid

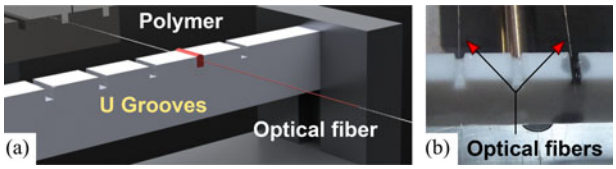

Fig. 3. Details of the U-grooves used as liquid reservoirs for the coating system: (a) illustration and (b) photograph of the reservoir and the fibers during the coating process.

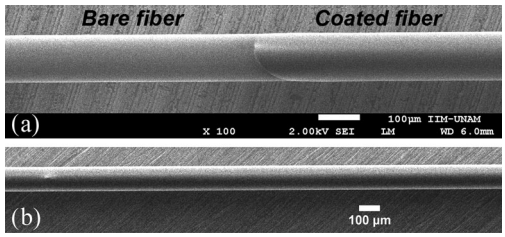

Fig. 4. Scanning electronic microscopy (SEM) images of an optical fiber coated with UVpoly layer of approximately 1.15 μm at a speed of 1 mm/min: (a) initial section of the coating and (b) uniformly coated optical fiber (bright dot caused by sample preparation-manipulation for SEM imaging).

swaging. For the case of tapered fibers, these are placed in the machine using a special holder maintaining same tension resulting after the tapering process. The grooves on this metallic bars are aligned with the PTFE reservoirs with the capability of placing up to ten fibers/capillaries for simultaneous coating.

IV. Coating Thickness Characterization

Standard single-mode optical fibers with a diameter of 125 μm (Corning SMF-28e) and 20 μL glass capillary tubes (Drummond, 450.85 μm radius) were used to characterize the coating process. The coating materials were polydimethilsiloxane (PDMS, Sylgard 184) and an acrylate UV curing polymer (Efiron PC-414, further denoted as UVpoly). An optical fiber coated with UVpoly is shown in Fig. 4; while the difference between the bare fiber and the coated section is clearly noticeable in Fig. 4(a), the uniformity of the resulting coating is demonstrated in Fig. 4(b). The performance of the coating system using both, optical fibers and glass capillaries, was evaluated upon using different values for the relevant parameters involved in the process (i.e., coating speed and viscosity of the coating). We further evaluated the capability for obtaining coatings with multiple layers.

A. Single Layer Coatings on Optical Fibers

Optical fibers were coated with thin layers of PDMS and the UVpoly in 35 mm long sections and at different speeds. Subsequently, the increase in diameter due to the deposited coating layers was measured using scanning electron microscopy (SEM). SEM images were analyzed in sections of 215 μm in length, every 5 mm along the entire coated section of the fiber. Direct comparison of these images with those obtained from an uncoated section of the fiber yielded the increase in fiber diameter due to the deposited coating layer. In order to avoid fluid instabilities, the fibers were coated at low velocities (<2 mm/min); thus, thin and uniform polymer layers were readily obtained.

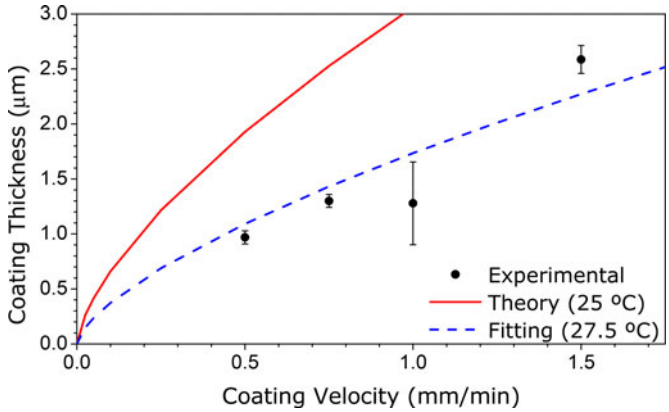

Fig. 5. Measured layer thicknesses for the UVpoly at different coating velocities and calculated thickness for two different temperatures.

The thickness of the coating obtained with the UVpoly for different velocities (0.5, 0.75, 1.0, and 1.5 mm/min) is shown in Fig. 5. Polymer curing was carried out once the coating process was finished; this was done with an UV curing LED system (Thorlabs CS2010) centered at a wavelength of 365 nm with a power density of 6 W/cm^2, on a single sweep across the coated length, for a period of time of 2 min. Comparison of the experimental thicknesses with the LLD theory requires a proper calculation of the Capillary number. Since the data sheet of the UVpoly only provides the values of the viscosity as a function of temperature, we estimated the surface tension by fitting Eq. (1) with the experimental data. It is important to notice that both, surface tension and viscosity, are highly affected by temperature and this in turn will affect the resulting coating thickness. In our case, the experiments were performed at a room temperature of 27.5 °C, which yields an estimated viscosity of 6.45 Pa/s for the UVpoly. The fitting using (1) yields a surface tension of 36.09 mN/m, which is in good agreement with previous reports for acrylate polymers [21]. The standard deviation observed in the experimental results is attributed to thermal variations during the coating process. For comparison, Eq. (1) is also plotted in Fig. 5 for a room temperature of 25 °C.

The characterization of the PDMS coatings required a more elaborated procedure owing to the curing mechanism of this polymer. Being a thermally curable material, the surface tension and the viscosity of PDMS vary with time; thus, different conditions occur during the coating process. In addition, the PDMS properties are also dependent on the mixture ratio of base polymer and curing agent. As an example, the data sheet specifies a $\mu = 5.1$ Pa/s for the base polymer and a $\mu = 3.5$ Pa/s for a mixture ratio of 10:1 [22]. For the same ratio of polymer to curing agent, a $\gamma = 19.8$ mN/m is reported elsewhere [23].

In order to consider appropriate values of viscosity for the mixture ratio used in our experiments (8:1 polymer to curing agent), a time-dependent rheological characterization of

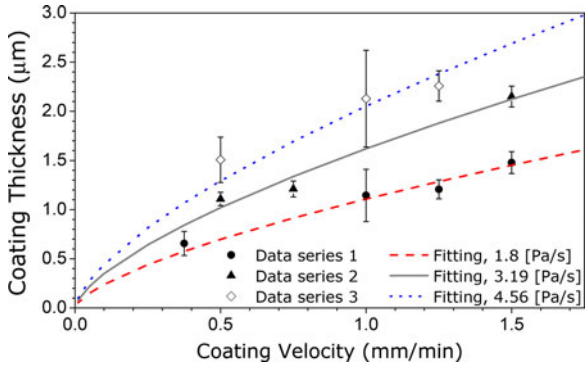

Fig. 6. Characterization of the coating layer thickness for the PDMS at different coating velocities and viscosities.

the PDMS was carried out (ARG2 rheometer, TA Instruments, cone-plate geometry 60 mm, 2°). This yielded a nearly Newtonian viscosity of 0.5 Pa/s for a temperature of 27.5 °C during the first half hour after the mixture was done. However, after four hours the viscosity of the mixture was measured again and a $\eta = 10$ Pa/s was obtained, showing a large dependence of its properties during the curing process.

Several bare optical fibers previously cleaned with laboratory grade isopropyl alcohol and acetone were coated with PDMS using a mixture ratio of 8:1 at different velocities ranging from 0.375 to 1.5 mm/min. As before, the coating thickness was measured via SEM images. Results are shown in Fig. 6 illustrating the different thicknesses attainable for the same coating velocity but with different viscosities. The corresponding fitting curves, obtained considering a $\gamma = 19.8$ mN/m, are also included to demonstrate the effects of the increase in viscosity on the expected PDMS coating thicknesses. As seen in the figure, the layer thickness increases with the polymer viscosity; this in turn is noticeably affected by thermal fluctuations and which also evolves in time. Therefore, for thermally activated polymeric coatings solidifying at room temperature, it is recommended to always start the coating process immediately after adding the curing agent. This action will ensure that the coating layer will be deposited during the lapse of time where the polymer maintains a constant viscosity and homogeneity. As an example, the difference in error bars shown in some experimental points of Figs. 5 and 6 can be attributed to changes in viscosity of the polymer mixtures. In some of these cases, the polymers were prepared in different days under different environmental conditions. Nonetheless, the results seem to be consistent with the predictions of wire coating theory.

Thin layers of both polymeric materials were deposited on optical fibers to observe the suitability of the system for devices with small diameters such as tapers and fiber fused couplers. The thickness of the layers was successfully controlled upon adjusting the coating velocity according to the features of the applied polymer. Using the fitted values of the surface tension, the Bond numbers calculated in our experiments yield values of 1.6×10^{-3} for the UVpoly and 4.9×10^{-3} for the PDMS. Thus, for both cases, gravity effects on the coatings are negligible and radial uniformity can be assumed.

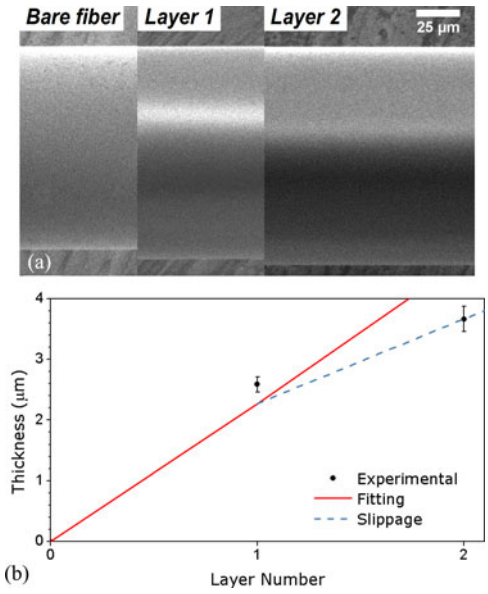

Fig. 7. Characterization of the layer thickness of UVpoly for multiple layers on optical fibers: (a) SEM images of the bare and coated fibers; (b) measured thicknesses for the layers and fitting using the slipping condition (see text).

SEM images showed that uniform coatings over the entire length of the fibers are readily obtained, even for devices of a few centimeters in length. This is an important feature for tapered fiber optic devices, since non-uniform coatings may lead to high transmission losses. As we will demonstrate in subsequent sections, the proposed coating system is suitable for developing polymer coated fiber optic devices.

Notice that for tapered devices, the transition region will develop a variable coating thickness owing to its direct dependence on the fiber radius (see Eq. (1)). For a constant coating velocity, gradually tapered devices will have a thinner coating layer as the fiber radius decreases. Aside from thermal effects, other contributions that may alter the coatings thickness and uniformity include external vibrations and humidity. These should therefore be minimized and particularly during coating layer deposition.

B. Multilayer Coatings

Optical devices requiring thicker layers of polymer can also be fabricated upon performing a multiple coating process. Notice that this procedure prevents the decrease in growth time of the surface instability, which involves an increase in the thickness h. This approach was explored by applying multiple layers of the described polymers onto optical fibers and glass capillaries. The fibers were coated at a speed of 1.5 mm/min with one layer of UVpoly, and after curing with UV light irradiation, a second layer of the same polymer was deposited and cured. The results are shown in Fig. 7(a), in which an increase in fiber diameter is clearly observed for a two-layer coating. It is important to notice that for multiple layers, the LLD thickness model (Eq. (1)) requires adjustments due to a possible slipping condition. This arises from the fact that subsequent layers will

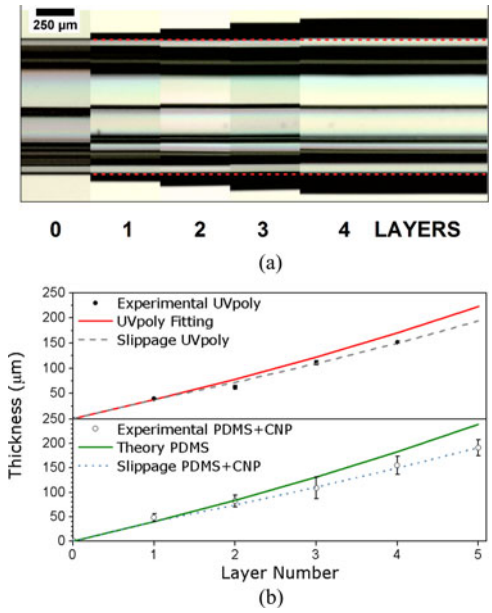

Fig. 8. Characterization of the coating layer thickness for the UVpoly for multiple layers on glass capillaries: (a) optical microscopy pictures of the coated capillary (dashed line indicates the capillary original diameter), (b) experimental data obtained from experiments; data of PDMS + CNP coatings were taken from reference [26].

be deposited on a solid polymer–liquid polymer interface (i.e., liquid polymer over a cured polymer) instead of having a glass-liquid polymer interface, thereby favoring slippage of the liquid [24]. Slippage during coating can be accounted for using an "apparent viscosity" given by [25]:

$$n_{\mathrm{app}} = \frac{\eta h}{(h + \lambda_{\mathrm{slip}})} \tag{5}$$

where λ_{slip} is the slip length, which accounts for the non-zero velocity at the interface. Using Eqs. (1) and (5) we obtained a $\eta_{\mathrm{app}} = 2.93$ Pa/s and a $\lambda/h = 1.2$; as shown in Fig. 7(b), the thickness of the second layer coating agrees well with the value predicted by the LLD model considering the apparent viscosity.

Recently, the use of photoresponsive layers on glass capillaries has been proposed as a novel approach for inducing thermocapillary flow [26]. Therefore, it is of interest to evaluate the performance of the coating system for applying multiple coating layers on the outer surface of glass capillary tubes. The corresponding Bond numbers for the capillaries are 0.085 for the UVpoly and 0.10 for the PDMS; as before, gravity effects on the coating layers are minimum. The glass capillaries were coated with the UVpoly at a velocity of 5.21 mm/min and the results were compared with those previously reported for multiple layers of PDMS with carbon nanopowder (PDMS-CNP). As seen in Fig. 8, a lower slippage is obtained for the UVpoly, with a $\eta_{\mathrm{app}} = 5$ Pa/s and a $\lambda/h = 0.29$. For the PDMS-CNP composite, the fitting yields a $\eta_{\mathrm{app}} = 2.7$ Pa/s and a $\lambda/h = 0.44$. Measurements of layer thicknesses in this case were performed by optical microscopy. As expected, thicker coatings will be less affected by the variations caused by the apparent viscosity and hence slippage will decrease (i.e., $\eta_{\mathrm{app}} = \eta$, see Eq. (5)).

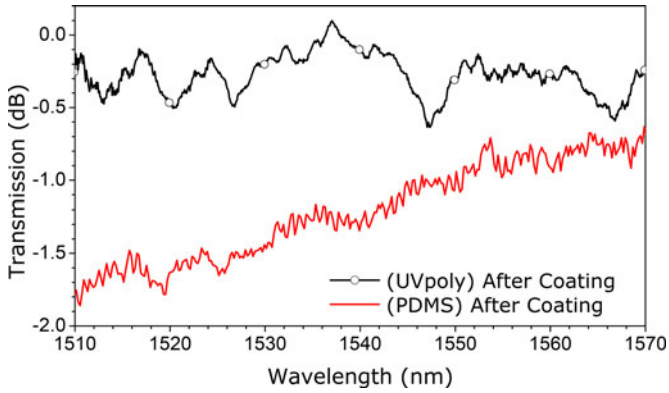

Fig. 9. Transmission losses registered after coating tapered optical fibers.

As shown above, multiple layer coatings can be readily deposited on devices ranging from the micrometric to millimetric diameter scales. It is important to notice that the desired thickness of each layer can be easily adjusted upon controlling the coating process velocity following the guidelines provided by simple wire coating theory.

V. Optical Characterization and Applications

The optical losses induced by the coatings were evaluated on the transmission spectra of tapered optical fibers. These were fabricated with standard single-mode fibers using the flame-brush technique [27]. Tapers with a constant waist diameter of approximately 6 μm along 1 cm and length of 4 cm, were coated at a speed of 1.5 mm/min using both, the UVpoly and PDMS, yielding coating layers with thicknesses of 200 and 110 nm, respectively. The attenuation losses registered on the transmission once the layers were deposited onto the tapered section of the fibers are shown in Fig. 9. For PDMS, the losses generated by the coating layers can vary from 1.8 to 0.75 dB, while for the UVpoly they can reach 0.75 dB. The observed spectral modulation can be attributed to the change in refractive index of the surrounding media on the tapered sections of optical fibers, as well as to mode confinement when a layer with similar refractive index surrounds the optical fiber material. The observed attenuation slope can be explained as a wavelength dependent power confinement variation due to the change of the coating refractive index. Also, in both cases small perturbations are registered with maximum amplitude of 0.3 dB, which may be attributed to modal beating observed in non-adiabatic tapered structures [28]–[30]. This therefore suggests that small non-uniformities are present along the coating layer, caused by the impurities of the polymers and the growth of instabilities.

A direct application for the coating system of potential interest to microfluidics has been reported elsewhere using glass capillaries [26]. We now demonstrate its use for the fabrication of optical fiber devices. Overcoupled fused fiber couplers have been used as wavelength tunable filters when the refractive index of the coupling region changes due to thermal effects achieved via an electrical heater [31]. The effects of this process are usually improved encapsulating the coupler inside a

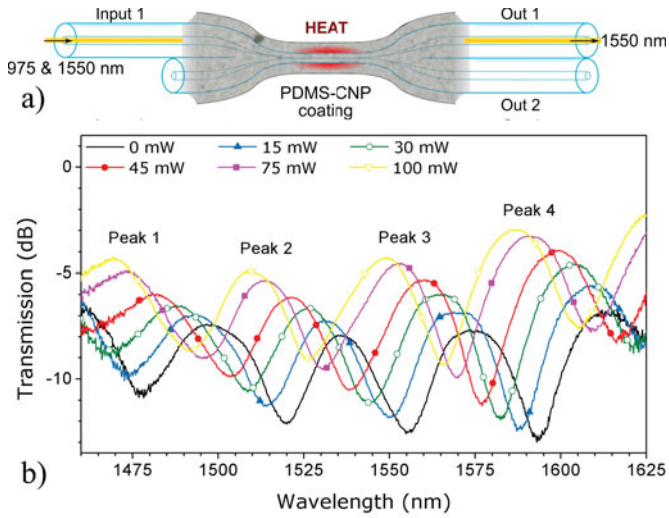

Fig. 10. Optical fiber device coated with PDMS-CNP using the coating system. (a) Experimental setup and scheme of the device. (b) Transmission spectra as function of pump power.

polymer with a larger thermo-optic coefficient [32]. We fabricated a fused overcoupled coupler and then coated it with a PDMS-CNP composite (see Fig. 10(a)) [33]. The mixture of PDMS-CNP was fabricated using a concentration of 1 mg/g and a coating layer of approximately 750 nm was applied onto the coupling region. For this coating material, the thermal effect is generated via optical absorption of the CNP and this in turn changes the refractive index of the PDMS layer [32]. Hence, an optically tunable fiber optic coupler can be realized.

Two light sources at different wavelengths were fed to the optical coupler using a WDM: a laser diode (LD, 200 mW max. output power) operating at 975 nm and a LED centered at 1550 nm with a 100 nm full-width at half-maximum. While the LD is used as the control signal to induce the refractive index changes in the coupling region, the LED is used as the probe beam to register changes in the transmission spectrum of the device via an optical spectrum analyzer. The spectra registered when increasing the power of the LD from 0 to 100 mW are shown in Fig. 10(b). Analysis of the shift for each lobe as a function of pump power reveals wavelength displacements of 0.32, 0.26, 0.23, and 0.26 nm/mW. Notice that the shifts in the peak wavelengths are very similar in all cases, and the observed differences may be attributed to mode confinement conditions. The optical absorption of the CNP at the LD wavelength generates a change in the refractive index of PDMS mediated by thermal effects, thus creating a local change in the effective refractive index. Notice also that the thermo-optic coefficient of the PDMS ($\mathrm{d}n/\mathrm{d}T = -4.5 \times 10^{-4}/°\mathrm{C}$) is larger than that of silica, air, and other materials previously used for this type of device [34].

VI. Conclusion

We have demonstrated a system for applying polymer coatings on cylindrical devices with photonic applications. The performance and capabilities of the system were verified upon obtaining different thicknesses of polymer coatings simply by varying the speed of the coating process. Glass devices such as optical fibers and capillaries were successfully coated with two different polymers, thereby demonstrating the versatility of the proposed system. As demonstrated in our experiments, the thickness of the applied coatings can be conveniently predicted by wire coating theory, and the physical properties of the coating materials (e.g., viscosity and surface tension) play a key role on the estimation accuracy of the coating thickness. We further demonstrated that multiple layer coatings can also be realized, and the thickness for each layer can be estimated upon considering the slipping condition in wire coating theory. As shown with the overcoupled fiber optic coupler, the coating system provides a means for the fabrication of optical devices. Other functional polymers may be incorporated onto tapered devices and further optical functions may be realized via controlled deposition of polymer layers.

Acknowledgment

The authors would like to thank technical assistance from O. Novelo for acquiring the SEM images; useful discussions with M. Hautefeuille are also appreciated.

References

[1] M. Smietana, M. L. Korwin-Pawlowski, W. J. Bock, G. R. Pickrell, and J. Szmidt, "Refractive index sensing of fiber optic long-period grating structures coated with a plasma deposited diamond-like carbon thin film," *Meas. Sci. Technol.*, vol. 19, no. 8, p. 085301, Jun. 2008.

[2] L. Cheng-Ling, "Spectral analysis of waveguide tapered microfiber with an ultrathin metal coating," *Opt. Exp.*, vol. 18, no. 14, pp. 14768–14777, Jun. 2010.

[3] M. A. Butler and D. S. Ginley, "Hydrogen sensing with palladium coated optical fibers," *J. Appl. Phys.*, vol. 64, no. 7, pp. 3706–3712, Oct. 1988.

[4] L. E. Scriven, "Physics and applications of dip coating and spin coating," *Mater. Res. Soc. Symp. Proc.*, vol. 121, 1988, pp. 717–729.

[5] C. R. Zamarreño, P. Sanchez, M. Hernaez, I. Del Villar, C. Fernandez-Valdivielso, I. R. Matias, and F. J. Arregui, "Sensing properties of indium oxide coated optical fiber devices based on lossy mode resonances," *IEEE Sensors J.*, vol. 12, no. 1, pp. 151–155, Jan. 2012.

[6] V. A. Márquez-Cruz and J. A. Hernández-Cordero, "Fiber optic Fabry–Perot sensor for surface tension analysis," *Opt. Exp.*, vol. 22, no. 3, pp. 3028–3038, 2014.

[7] B. J. Cronk *et al.*, "High reliability, automated fiber recoat process that increases fiber recoating yields," presented at the NEPCON West Fiberopt. Exp., CA, USA, Dec. 2005.

[8] S.-M. Chuo and L. A. Wang, "Propagation loss, degradation and protective coating of long drawn microfibers," *Opt. Commun.*, vol. 284, no. 12, pp. 2825–2828, Jun. 2011.

[9] S. R. Schmid and A. F. Toussaint, "Optical fiber coatings," *Specialty Optic Fibers Handbook*, A. Mendez and T. F. Morse, Eds. Amsterdam, The Netherlands: Elsevier, pp. 95–122, 2007.

[10] G. Y. Chen, M. Ding, T. P. Newson and G. Brambilla, "A review of microfiber and nanofiber based optical sensors," *Open Opt. J.*, vol. 7, Suppl. 1, pp. 32–57, 2013.

[11] N. Díaz-Herrera, M. C. Navarrete, O. Esteban, and A. González-Cano, "A fibre-optic temperature sensor based on the deposition of a thermochromicmaterial on an adiabatic taper," *Meas. Sci. Technol.*, vol. 15, no. 12, pp. 353–358, Feb. 2004.

[12] M. C. Ertan-Lamontagne, S. R. Lowry, W. R. Seitz, and S. A. Tomellini, "Polymer-coated tapered cylindrical ATR elements for sensitive detection of organic solutes in water," *Appl. Spectrosc.*, vol. 49, no. 8, pp. 1170–1173, 1995.

[13] G. Kakarantzas, S. G. Leon-Saval, T. A. Birks, and P. St. J. Russell, "Low-loss deposition of sol gel-derived silica films on tapered fibers," *Opt. Lett.*, vol. 29, no. 7, pp. 694–696, 2004.

[14] Z. Y. Xu, Y. H. Li, and L. J. Wang, "A versatile technique to functionalize optical microfibers via modified sol-gel dip-coating method," *Opt. Lett.*, vol. 39, no. 1, pp. 34–36, 2014.

[15] H. Ma, A. K.-Y. Jen, and L. R. Dalton, "Polymer-based optical waveguides: Materials, processing, and devices," *Adv. Mater.*, vol. 14, pp. 1339–1365, 2002.
[16] L. D. Landau and B. Levich, "Dragging of a liquid by a moving plate," *Acta Physicochem. URSS*, vol. 17, pp. 42–54, 1942.
[17] A. D. Ryck and D. Quéré, "Inertial coating of a fibre," *J. Fluid Mech.*, vol. 311, pp. 219–237, 1996.
[18] D. Quéré, "Fluid coating on a fiber," *Annu. Rev. Fluid Mech.*, vol. 31, pp. 347–384, 1999.
[19] D. A. White and J. A. Tallmadge, "A theory of withdrawal of cylinders from liquid baths," *AIChE J.*, vol. 12, no. 2, pp. 333–339, Mar. 1966.
[20] L. Rayleigh, "On the instability of jets," *Proc. London Math. Soc.*, vol. 10, pp. 4–13, 1878.
[21] B. Magny, S. Pelletier, G. Albrighton, and G. Eisele, "Importance of monomer interfacial tension for UV curable Litho Inks performance," presented at the RadTech Conf., Indianapolis, IN, USA, 2002.
[22] (Apr., 2014). *Sylgard184 Silicone Elastomer: Product Information-Electronics*, Dow Corning Co., USA. [Online]. Available: http://www.dowcorning.com/DataFiles/090276fe80190b08.pdf
[23] S. Wu, "Calculation of interfacial tension in polymer systems," *J. Polymer. Sci. C*, vol. 34, no. 1, pp. 19–30, 1971.
[24] R. Zhao and C. W. Macosko, "Slip at polymer–polymer interfaces: Rheological measurements on coextruded multilayers," *J. Rheol.*, vol. 46, pp. 145–167, 2002.
[25] L. Ying-Chih, L. Yen-Ching, and W. Hsien-Hung, "Drastic changes in interfacial hydrodynamics due to wall slippage: Slip-intensified film thinning, drop spreading, and capillary instability," *Phys. Rev. Lett.*, vol. 111, no. 13, p. 136001, 2013.
[26] J. R. Vélez-Cordero, A. M. Velázquez-Benítez, and J. Hernández-Cordero, "Thermocapillary flow in glass tubes coated with photoresponsive layers," *Langmuir*, vol. 30, no. 18, pp. 5326–5336, 2014.
[27] T. A. Birks and Y. W. Li, "The shape of fiber tapers," *J. Lightw. Technol.*, vol. 10, no. 4, pp. 432–438, Apr. 1992.
[28] A. A. Tovar and L. W. Casperson, "Beam propagation in parabolically tapered graded-index waveguides," *Appl. Opt.*, vol. 33, no. 33, pp. 7733–7739, 1994.
[29] X. Daxhelet, L. Martineau, and J. Bures, "Influence of the fiber index profile on vectorial fiber modes and application to tapered fiber devices," *J. Lightw. Technol.*, vol. 23, no. 5, pp. 1874–1880, 2005.
[30] R. J. Black, S. Lacroix, F. Gonthier and J. D. Love, "Tapered single-mode fibres and devices—Part 2: Experimental and theoretical quantification," *IEE Proc. J. Optelectron.*, vol. 138, no. 5, pp. 355–364, Oct. 1991.
[31] S. P. Shipley and A. El Fatatry, "All- single-mode optical fibre wavelength-tunable WDM with very narrow pass/stopband separations," *Electron. Lett.*, vol. 23, no. 10, pp. 523–524, 1987.
[32] K. T. Kim, K. J. Cho, and B. H. Lee, "Empirical analysis of widely tunable fused fiber coupler assisted by external medium of high thermo-optic coefficient," *Fiber Integr. Opt.*, vol. 30, no. 1, pp. 61–72, 2011.
[33] A. Velazquez-Benitez and J. Hernández-Cordero, "Optically controlled wavelength tunable fused fiber coupler," presented at the Workshop Specialty Opt. Fibers Appl., Sigtuna, Sweden, Aug. 2013, Paper W3.25.
[34] C. Markos, K. Vlachos, and G. Kakarantzas, "Guiding and thermal properties of a hybrid polymer-infused photonic crystal fiber," *Opt. Mater. Exp.*, vol. 2, no. 7, pp. 929–941, 2012.

Amado M. Velázquez-Benítez received the B.Sc. and M.S. degrees in electrical engineering (electronics) in 2010 and 2012, respectively, from the Engineering School, National Autonomous University of Mexico, Mexico City, Mexico, where he is currently working toward the Ph.D. degree in engineering. He is currently carrying out research in fiber sensors at the Fiber Lasers and Fiber Sensors Laboratory, IIM, UNAM.

Moisés Reyes-Medrano, biography not available at the time of publication.

J. Rodrigo Vélez-Cordero received the Ph.D. degree in materials science and engineering and the M.S. degree in biochemical engineering from UNAM, México. He spent a year as a postdoctoral fellow in the Mechanical and Aerospace Engineering Department at UC San Diego under the grant UC-MEXUS. His research interests include the interaction of micronanoparticles with light, structure-rheology of soft matter, microhydrodynamics.

Juan Hernández-Cordero received the B.Sc. degree in electrical engineering from the National Autonomous University of Mexico, Mexico City, Mexico, in 1992, and the M.S. and Ph.D. degree in engineering from Brown University, Providence, RI, USA, in 1996 and 1998, respectively. After completing a year as a Research Assistant with the Materials Research Institute, UNAM, he was awarded a full scholarship to pursue graduate studies at Brown University. He then spent a year as a Postdoctoral Research Associate with the Laboratory for Lightwave Technology, Boston University. He is currently with the IIM, UNAM, where he has established the Fiber Lasers and Fiber Sensors Laboratory. His fields of interest include optical fiber sensors, fiber lasers, and fiber devices.